energies

MDPI

Article

Networking Strategy of Small Hydropower Microgrid Under Weak Communication Conditions

Zhifeng Chen [1], Zifan Zhang [1,*], Zhanhong Liang [2,3], Yuan Tang [1,4] and Na Shen [1]

[1] Department of Electrical Engineering, Guangzhou City University of Technology, Guangzhou 510080, China; chenzf@gcu.edu.cn (Z.C.)
[2] CLP Power Hong Kong Ltd., Hong Kong 999077, China
[3] Department of Electrical Engineering, City University of Hong Kong, Hong Kong 999077, China
[4] School of Electric Power, South China University of Technology, Guangzhou 510641, China
* Correspondence: zhangzif@gcu.edu.cn; Tel.: +86-135-7023-6228

Abstract

Small hydropower-dominated microgrids enable power exchange with the main grid during grid-connected operation but face frequency stability challenges during sudden islanding (e.g., line faults), requiring prompt generation curtailment or load shedding. In communication-constrained mountainous regions, conventional methods such as high-frequency tripping or low-frequency load shedding often struggle to achieve precise frequency regulation A hierarchical strategy integrating master station centralized decision making and substation local control is proposed. This study theoretically analyzes the post-islanding frequency dynamics of small hydropower microgrids. The master station formulates optimal shedding decisions using regional power flow data, while substations execute decisions via local measurements to mitigate communication issues. A constrained mathematical model is established, solved using a heuristic algorithm, validated through electromagnetic transient simulations, and compared with traditional schemes. The proposed scheme achieves precise surplus capacity shedding, enhancing frequency stability during abrupt islanding with reduced over-/under-tripping compared to that of conventional methods. This hierarchical strategy enhances frequency regulation capability under communication constraints, ensuring reliable operation of small hydropower microgrids during sudden islanding and providing a practical solution for remote regions with limited communication infrastructure.

Keywords: small hydropower; island operation; microgrid; frequency; weak communication

check for updates

Academic Editor: José Matas

Received: 2 July 2025
Revised: 12 August 2025
Accepted: 15 August 2025
Published: 20 October 2025

Citation: Chen, Z.; Zhang, Z.; Liang, Z.; Tang, Y.; Shen, N. Networking Strategy of Small Hydropower Microgrid Under Weak Communication Conditions. *Energies* **2025**, *18*, 5518. https://doi.org/10.3390/en18205518

Copyright: © 2025 by the authors. Licensee MDPI, Basel, Switzerland. This article is an open access article distributed under the terms and conditions of the Creative Commons Attribution (CC BY) license (https://creativecommons.org/licenses/by/4.0/).

1. Introduction

As a clean distributed energy source, small hydropower features low investment costs, long operational life, and strong adaptability to diverse tasks (e.g., power generation and frequency regulation), thus demonstrating excellent overall performance [1]. Therefore, small hydropower stations are widely distributed in regions with abundant water resources [2]. The power generation of small hydropower stations is directly related to the flow rate and head of the river. Small hydropower stations are typically located in remote areas and are more extensively integrated into the power system compared to rural distribution networks [3,4].

The construction of power transmission channels for rural power grids usually lags behind the growth of power generation capacity, resulting in weak connections between some regional grids and the main network [5–7]. For example, if a single interconnection

transformer or single circuit line is connected to the network, the fault tripping of the interconnection element will cause some power grids to be separated from the main network, forming an islanded operation. For hydropower units in islanded operation, the current handling method is relatively simplistic: hydropower units are tripped immediately after islanding. After faulty components are repaired and power supply is restored, the grid connection is reestablished through the stepwise restart of hydropower units [8,9]. To make full use of renewable power sources and improve the reliability of the power supply, the isolated island of the regional power grid containing small hydropower, hydropower clusters, and local load is used to form a microgrid that can operate independently [10]. This scheme can improve the ability of the power grid to deal with sudden failures and avoid large-scale blackouts caused by some component failures [11].

The local power load of the regional power grid connected with small hydropower stations is usually small. After meeting the local load demand, the hydropower power generation capacity is transmitted to the system through connecting elements, that is, the power transmission regional power grid. Such power-exporting grids will accumulate surplus power within the islanded range after islanding occurs, causing a rise in the operating frequency of the islanded system. Therefore, the biggest challenge for the stable operation of microgrids with small hydropower in a grid-isolated state is frequency stability.

At present, the common method of dealing with the frequency stability problem under the isolated operation state of the hydropower microgrid is to cut off the generator at high frequency, that is, when the frequency of the hydropower microgrid is too high, to cut off some units to keep the frequency stable [12,13]. High-frequency tripping typically initiates unit tripping when the frequency exceeds the threshold. However, the tripped generation capacity is often imprecise, leading to frequent over-tripping. Some studies propose accelerating generator tripping using the Rate of Change of Frequency (ROCOF) criterion: when the system frequency exceeds the first-round threshold of high-frequency tripping and maintains this state for a set delay, the frequency change rate (measured locally by units) is used to trigger additional tripping rounds [14–16]. This method can accelerate tripping, to a certain extent, but still lacks accuracy and predictability in regards to unit tripping.

This article proposes a control method of centralized decision making of the main station + on-site control of sub stations. The main station formulates strategies based on collected data, refreshes, and issues control instructions at certain time intervals (such as 1 s intervals). Substations perform local measurements and simple calculations to detect islanding events and generate a detection signal. The isolated discrimination signal is refreshed at regular intervals (such as 20 ms). The substation can formulate a strategy for whether to switch off the machine based on the main station information and local isolate information. This method exhibits low dependence on communication and can accurately and quickly achieve the disconnection of units or loads.

The main contributions of this paper are as follows:

1. A master station centralized decision making + substation local control method is proposed to address the challenge of precise unit tripping and load shedding during sudden islanding of small hydropower microgrids under weak communication conditions, ensuring post-islanding frequency stability.
2. The mathematical model of the decision problem is established by taking the microgrid frequency change into account, a heuristic algorithm is used to obtain the optimal solution for more effective control, and the effectiveness of this strategy is verified by simulation.

2. Principle Analysis of Frequency Variation in Isolated Hydropower Stations

To stabilize the frequency of islanded hydropower systems, understanding the frequency variation mechanism after islanding is essential, regardless of the load-shedding strategy adopted. It is necessary to fully study the frequency change mechanism of the regional power grid comprising hydropower after the occurrence of an isolated state.

The small and medium-sized hydropower generation capacity of the regional grid comprising rich hydropower is greater than the local load power consumption, and the hydropower microgrid becomes a power output grid when it is connected to the power grid. When the regional power grid containing hydropower is separated from the main power grid and enters into isolated operation, the surplus power cannot be sent out. If some hydropower units are not cut off in time, the frequency of the microgrid system operating in a grid isolated state will be too high.

2.1. Analysis of Frequency Change After Hydropower Microgrid Isolating

Most of the existing small hydropower stations in China are runoff hydropower stations. Water levels are raised to maximize water potential energy, enhancing energy conversion efficiency The transformation of runoff hydropower or the construction of a reservoir can form a reservoir-type small hydropower system to facilitate the regulation of water volume, regulating the output of small hydropower. The structure and energy change process of small hydropower systems are shown in Figure 1.

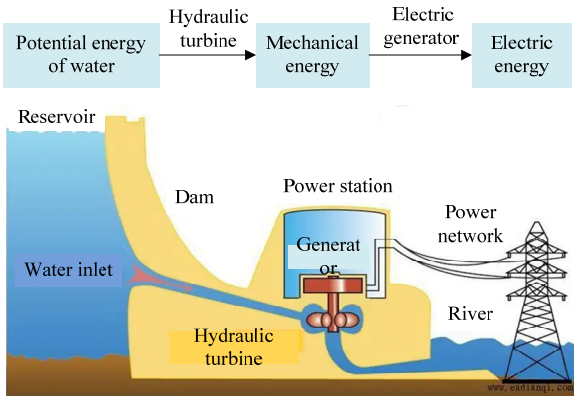


Figure 1. The energy conversion process of small hydropower.

The generator of a hydropower station is usually a synchronous generator. The input mechanical power and output electromagnetic power of the generator are equal. When the two torques are equal, the rotor rotates at a constant speed, and the hydroelectric microgrid maintains stable frequency operation. When the input torque is not equal to the output torque, the relationship between the generator rotor acceleration and the input and output power can be expressed as

$$\frac{d\omega}{dt} = \frac{1}{T_j}(T_m - T_e) \approx \frac{1}{T_j}(P_T - P_e) \quad (1)$$

where ω is the rotor angular velocity, $d\omega/dt$ is the rotor acceleration, P_e is the electromagnetic power, P_T is the mechanical power, T_j and is the inertia time constant of the generator, usually a fixed value.

It can be concluded from Formula (1) that when the microgrid is suddenly disconnected from the system, the power transmitted to the system before the hydropower microgrid is disconnected will not be transmitted due to isolation, resulting in a sudden

decrease in P_e. At the same time, the mechanical power P_T of the generator will not change suddenly due to the large inertia of the hydraulic turbine and generator, e.g., before the isolating, $P_T = P_e$, and after the isolating, $P_T > P_e$. The acceleration of the rotor is a positive value, that is, the generator speed is accelerated, which leads to high grid frequency.

Small hydropower stations often lack frequency modulation capability due to budget constraints and turbine design limitations [17]; even those with basic regulation functions cannot handle large frequency deviations from sudden islanding, necessitating active load/generation shedding. However, the large frequency deviation caused by sudden isolation exceeds the Frequency Modulation (FM) capability of the equipment. At this time, it is necessary to cut off the machine to ensure frequency stability in the grid-isolated state.

2.2. Mechanism Analysis of Smooth Switching in Hydroelectric Microgrids

The power balance in the microgrid is the key factor to ensure the stable operation of the system. To deal with the frequency impact caused by sudden isolation on the hydropower microgrid, it is critical to issue shutdown commands promptly upon islanding detection. Internal power balance enables the microgrid to achieve seamless transition during islanding; pre-formulated load-shedding strategies ensure frequency and voltage stability within allowable ranges. Take the simple system shown in Figure 2 as an example to analyze the smooth switching mechanism of the microgrid.

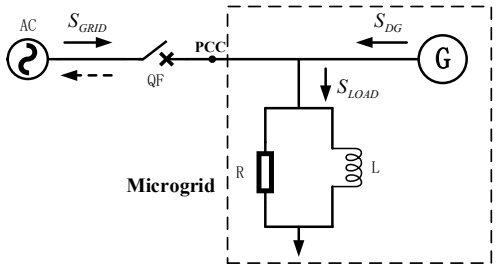


Figure 2. Schematic diagram of microgrid smoothing mechanism analysis.

When the microgrid is connected to the grid under normal conditions, small hydropower and the superior grid may supply power to the load simultaneously. In addition to supplying power to loads, small hydropower also supplies power to the superior power grid. Thus, the power distribution in the microgrid conforms to the following relationship:

$$\begin{cases} P_{LOAD} = \frac{U^2}{R} = P_{DG} \pm P_{GRID} \\ Q_{LOAD} = \frac{U^2}{2\pi f L} = Q_{DG} \pm Q_{GRID} \end{cases} \tag{2}$$

where P_{LOAD}, Q_{LOAD} represents the load active power and reactive power during normal grid connection; P_{DG}, Q_{DG} is the power provided by small hydropower during normal grid connection; P_{GRID}, Q_{GRID} is the power provided by the superior power grid during normal grid connection; U, f are, respectively, the voltage and frequency at the point of common coupling (PCC) of the grid connection point during normal grid connection; R, L is the equivalent resistance and inductance of the load.

When the interconnection switch at the PCC point is disconnected, and the connection between the microgrid and the superior grid is interrupted due to power outage maintenance or line fault and other events on the superior grid, only small hydropower supplies power to the load independently, and the following formula is valid:

$$\begin{cases} P'_{LOAD} = \frac{U'^2}{R} = P'_{DG} \\ Q'_{LOAD} = \frac{U'^2}{2\pi f' L} = Q'_{DG} \end{cases} \tag{3}$$

where P'_{LOAD} and Q'_{LOAD}, respectively, represent the active power and reactive power of load during isolate operation; P'_{DG}, Q'_{DG} provide power for distributed power supply during isolate operation; U and f, respectively, represent the voltage and frequency at the parallel point PCC during isolate operation.

If there is no sudden change in the power provided by the distributed power generation after isolation, then

$$\begin{cases} P'_{DG} = P_{DG} \\ Q'_{DG} = Q_{DG} \end{cases} \tag{4}$$

Thus, after the system enters the isolated state, the voltage at the PCC point and system frequency are described by the following relationship:

$$\begin{cases} \frac{U}{U'} = \sqrt{1 + \frac{P_{GRID}}{P_{DG}}} \\ \frac{f}{f'} = (1 + \frac{Q_{GRID}}{Q_{DG}})\frac{U'^2}{U^2} = (1 + \frac{Q_{GRID}}{Q_{DG}})(\frac{1}{1+\frac{P_{GRID}}{P_{DG}}}) \end{cases} \tag{5}$$

When the power provided by the superior main network is close to zero, that is, when $P_{GRID} \approx 0, Q_{GRID} \approx 0$, there is

$$\begin{cases} U' \approx U \\ f' \approx f \end{cases} \tag{6}$$

It can be seen from the above analysis that when the microgrid is normally connected to the grid, if the internal source load of the microgrid is nearly balanced, the frequency and voltage during off-grid operation are almost the same as those during grid-connected operation, and the microgrid can stably operate in islanded operation. Then, if the isolate division strategy is formulated in advance, and the strategy is implemented at the moment of failure to ensure the internal power balance of the microgrid, the frequency and voltage of the microgrid will be stable within the allowable range, and the microgrid can be switched smoothly.

3. Methodology

In hydropower-rich regional grids, microgrids integrated with small hydropower and local loads typically operate in a power surplus state, functioning as power-exporting grids. During sudden islanding events, surplus power accumulation threatens system frequency stability, necessitating prompt removal of some hydropower units. Traditional high-frequency generator tripping schemes, however, suffer from limitations such as low control precision and prolonged response delays. To address these, this paper proposes a master station-based load and generator shedding strategy, enabling rapid and accurate surplus capacity removal to maintain frequency stability in islanded microgrids.

As analyzed in Section 2.2, voltage and frequency stability in islanded systems relies on internal power balance. To prevent excessive frequency elevation after disconnection from the main grid and ensure seamless transition from grid-connected to islanded operation, a hierarchical control strategy centered on the master station is proposed for small hydropower microgrids.

The master station formulates pre-optimized emergency islanding strategies at regular intervals based on real-time load data and operational information from each small hydropower unit, generating corresponding decision tables that are distributed to substations. Substations adjust initial control commands by integrating local islanding detection results with master station instructions. This master station centralized decision-making + substation local execution framework enables smooth transition of the hydropower microgrid from grid-connected to islanded operation, prioritizing continuous power supply to critical loads within the network.

Hydropower-rich regions are typically characterized by complex geographical environments, where communication primarily relies on wireless public networks, leading to low reliability in data transmission. The proposed master station centralized decision-making + substation local decision-making control mode is engineered to address such communication constraints: in cases of data loss or transmission delays from the master station, substations automatically resort to the most recently received decision table, which is critical, given that communication delays in weak networks can degrade secondary control performance [18]. Even when abrupt changes occur in the islanding trend of the hydropower microgrid, substations can still issue accurate generator-tripping commands by integrating the latest decision table with real-time local islanding detection results. This control mode thus demonstrates robust adaptability to application scenarios with communication delays, aligning with distributed strategies that enhance reliability under packet loss [19]. Its control architecture is depicted in Figure 3.

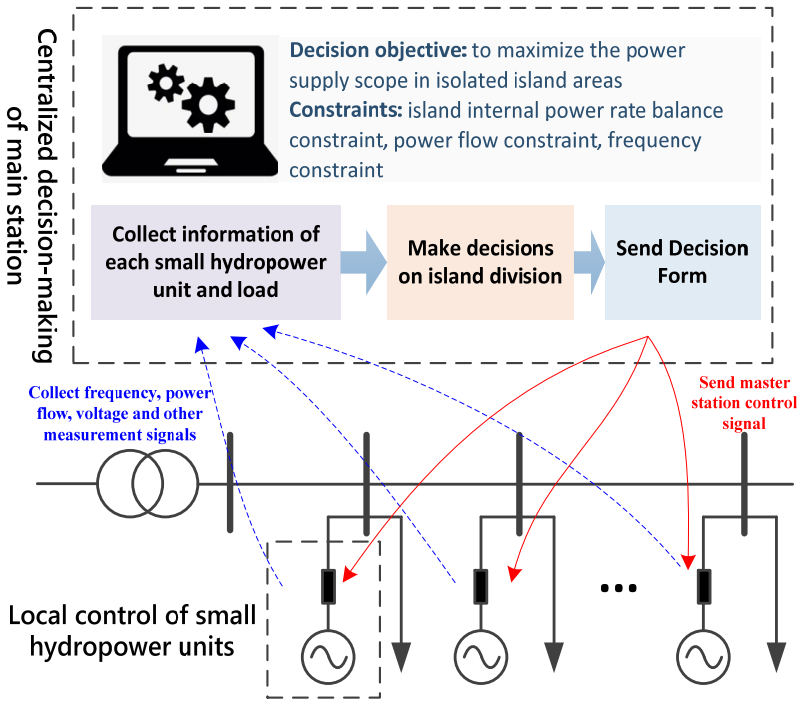


Figure 3. Control architecture of centralized decision + local control mode.

The master station collects electrical characteristics, such as frequency, power flow, and voltage, that characterize the system operation. By optimizing the decision, the decision table is sent to each small hydropower station.

The master station formulates control strategies based on collected operational data, incorporating communication delays, calculation delays, and control delays into its decision-making process. It sets a fixed refresh interval (e.g., 1 s) to update and issue control commands. Meanwhile, substations perform local measurements and real-time calculations to determine islanding status and generate corresponding detection signals, with the islanding judgment signal refreshed at a high-frequency interval (e.g., 20 ms). The operational workflow is illustrated in Figure 4.

Substations issue action instructions by integrating local islanding judgment results with the emergency off-grid decision table from the master station. If local detection confirms an islanding event, the corresponding hydropower units are tripped in accordance with the commands specified in the emergency off-grid decision table; if no islanding is detected, the system continues to operate in grid-connected mode.

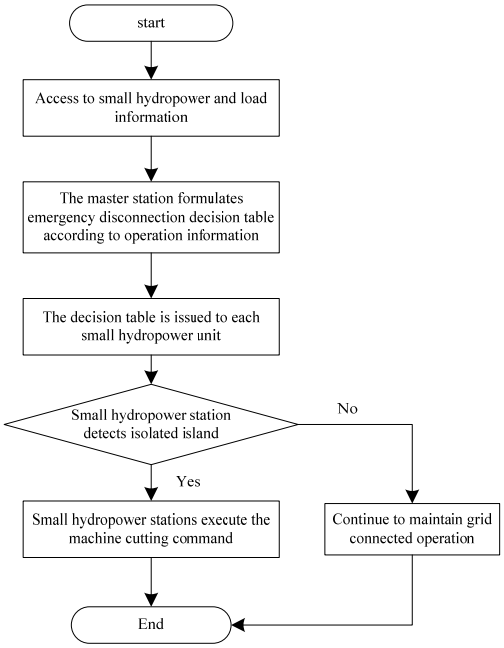


Figure 4. Centralized decision with local control flowchart.

4. Problem Formulation

4.1. Decision Model of Master Station

Ensuring frequency stability while minimizing the impact of power imbalance on the system is paramount for maintaining the stable operation of the microgrid after islanding. For power-exporting grids—where power supply typically exceeds local load demand—the core task during islanding events is to shed an appropriate number of hydropower units to rebalance supply and demand.

The decision-making process of the master station is governed by a well-defined objective function and corresponding constraints. The primary goal is to match the output of hydropower units as closely as possible to load demand while preserving adequate regulating capacity. The mathematical model proposed for this decision problem is formulated in Equations (7)–(13).

$$F = \min(\sum_{i=1}^{n} P_{G.i}(t) - \sum_{j=1}^{m} P_{load.j}(t)) > 0 \tag{7}$$

Dependent upon the output of each hydropower unit falling within its adjustment range.

$$P_{G.i_\min} \le P_{G.i}(t) \le P_{G.i_\max} \tag{8}$$

The frequency cannot exceed the following limit:

$$f_{\min} \le f(t) \le f_{\max} \tag{9}$$

A hydroelectric unit with regulation capability relies on adjusting the water intake of the turbine to regulate the mechanical power input to the hydroelectric unit. The mechanical power of the adjustable hydroelectric unit is

$$P_{m.i} = P_{m0.i} + \Delta P_{m.i} \cdot t \tag{10}$$

$$\Delta P_{m.i} = \begin{cases} 0.2P_{\text{N.i}} \text{ , } \sum P_{m.i} < \sum P_e \\ 0 \quad\quad\quad \text{, } \sum P_{m.i} = \sum P_e \\ -0.2P_{\text{N.i}} \text{, } \sum P_{m.i} > \sum P_e \end{cases} \tag{11}$$

The unit of rate of change of mechanical power $\Delta P_{m.i}$ is MW/s.

$$\Delta f = \int \frac{\sum P_{m.i} - \sum P_e}{2H_{hydro} \cdot S_{hydro}} f_{\text{N}} dt \tag{12}$$

f_{N} is the rated frequency, and Δf is the variation of frequency, which should be within the range of ± 5 Hz. $\sum P_{m.i}$ is the sum of the power of the small hydroelectric units; $\sum P_e$ is the sum of the loads; H_{hydro} is the inertial time constant of the hydropower isolate microgrid (the value is usually between 4.5 and 7); S_{hydro} is the system capacity of the hydropower isolate, numerically equal to $\sum P_{m.i} / \cos \varphi$; and the power factor is generally 0.85.

The voltage constraint condition of each node is

$$U_{\min} \leq U_i \leq U_{\max} \tag{13}$$

4.2. Optimization Process

In this study, a genetic algorithm (GA) is employed to solve the decision-making problem of island division for the master station.

The genetic algorithm, first proposed by John Holland in the United States in the 1970s, is a computational model derived from the evolutionary laws of natural organisms. It simulates the natural selection and genetic mechanisms described by Darwin's theory of biological evolution, serving as an optimization method to search for optimal solutions by mimicking natural evolutionary processes.

In this research, the output of hydropower generators is treated as an individual in the genetic algorithm, and a real-number encoding method is adopted for coding. If there are n variables constituting the vector $P_{g.i} = \{p_{g.1}, p_{g.2}, \ldots p_{g.n}\}$, the vector P could be seen as chromosome, and the vector $p_{g.i}$ could be seen as gene.

To design a real coding solution in genetic algorithms, the following steps are taken:

1. Establish an initial population.
2. Convert the objective function into a fitness function to evaluate the fitness of each individual in the population.
3. If any individual meets the predefined requirements in step 2, output the result and terminate the process.
4. If no eligible individual is found in step 2, proceed to the next genetic operations, i.e., selection, crossover, and mutation, to generate a new population.
5. Evaluate the fitness of each individual in the new population.
6. If there are individuals in the new population that meet the target criteria, output the result and terminate the process.

4.3. Genetic Algorithm Analysis

In this study, the genetic algorithm (GA) is employed to search for optimal combinations of small hydropower units and loads with regulable capacity. The experiments were conducted in the PyCharm Community Edition 2021.3.3 environment, using Python 3.9.

The initial population was defined as 25 binary-encoded individuals, with values ranging from 0 to $2^{25} - 1$. Each bit in the binary string represents the activation status of a corresponding feature: for example, the string "10101" indicates that the 1st, 3rd, and 5th features are activated, while the 2nd and 4th are deactivated.

To ensure system stability, constraints were imposed to limit the system frequency fluctuation to less than 0.5 Hz. Through iterative optimization, a set of combinations

satisfying the constraints and exhibiting regulable capacity was obtained. Analysis of the results confirmed that these combinations achieved a frequency fluctuation range within 0.5 Hz, meeting the predefined requirements.

This indicates that frequency significantly influences the regulable performance between small hydropower units and loads. By continuously adjusting parameter combinations, different regulation effects can be achieved, thereby effectively optimizing system performance. The GA-generated combinations of small hydropower units and loads that satisfy the constraints provide valuable insights for enhancing system performance optimization.

5. Case Study

To verify the effectiveness of the proposed strategy in stabilizing system frequency during sudden islanding, an electromagnetic transient simulation model was built using the PSCAD platform. The simulation system consists of 10 hydropower units and 15 loads connected via 10 kV lines, including 7 adjustable small hydropower units (G1–G7) and 3 non-adjustable small hydropower units (G8–G10), as shown in Figure 5. The output of hydropower units varies between wet and dry seasons (see Table 1), and the load power parameters are detailed in Table 2. The small hydropower microgrid connects to the superior power grid through the grid-connected circuit breaker BRK11.

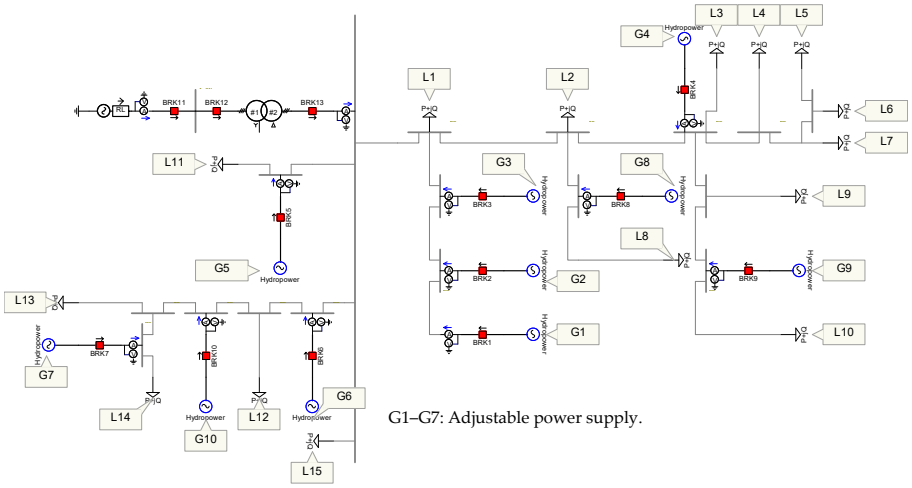


Figure 5. Main circuit diagram of the hydroelectric isolate simulation model.

Table 1. Rated capacity of small hydropower units in wet and dry season [MW].

Name	G1	G2	G3	G4	G5	G6	G7	G8	G9	G10	Total
wet season	0.5	0.525	1.5	0.84	0.85	1.65	0.9	0.57	0.44	0.1	7.875
dry season	0.35	0.4	0	0.5	0.6	0	0.54	0.3	0.27	0.06	3.02

Table 2. The data of loads [MW].

Name	L1	L2	L3	L4	L5	L6	L7	L8
Rated Capacity	0.33	0.23	0.15	0.08	0.18	0.6	0.5	0.18
Name	L9	L10	L11	L12	L13	L14	L15	
Rated Capacity	0.125	0.11	0.16	0.28	0.977	0.363	0.4	

5.1. No Machine-Cutting Scheme

When the small hydropower microgrid operates with power surplus, a system fault leading to disconnection from the superior power grid will cause a significant increase in system frequency, severely threatening operational stability and reliability.

The simulation waveform without any auxiliary control during islanding is shown in Figure 6. At 5 s after islanding, the system frequency surges to 57.62 Hz under the impact of isolation and eventually stabilizes around 54.45 Hz. This confirms that the uncontrolled scheme results in excessive frequency elevation during islanding, seriously impairing the stable and reliable operation of the power grid.

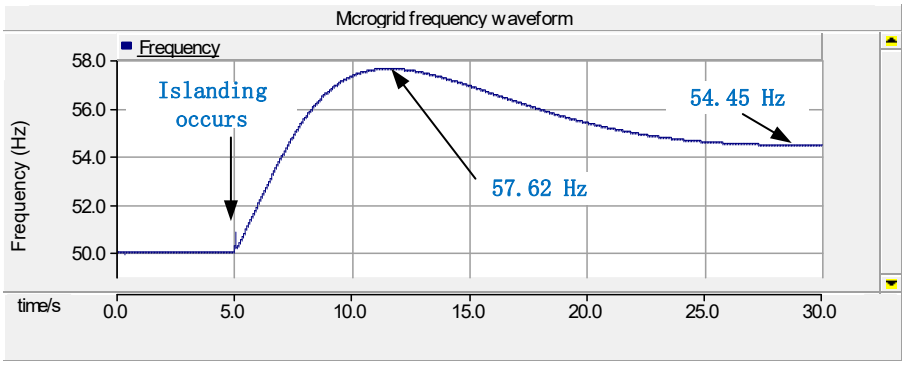


Figure 6. Simulation waveform without considering any auxiliary control.

5.2. Traditional Scheme: High-Frequency Generator-Shedding Strategy

High-frequency generator-shedding devices comprise the primary preventive measure to suppress continuous frequency elevation. These devices operate by sampling grid frequency values for logical judgment: when an abnormal frequency exceeding the threshold is detected, actuators independently perform load shedding or generator tripping [19]. For hydropower units, high-frequency protection typically integrates frequency and time elements, operating in staged sequences. As shown in Figure 7, the high-frequency shedding scheme is configured based on the maximum power deficit of the system or its components under extreme emergency conditions, with the ultimate goal of restoring frequency to the range of 49.5–50.5 Hz [20].

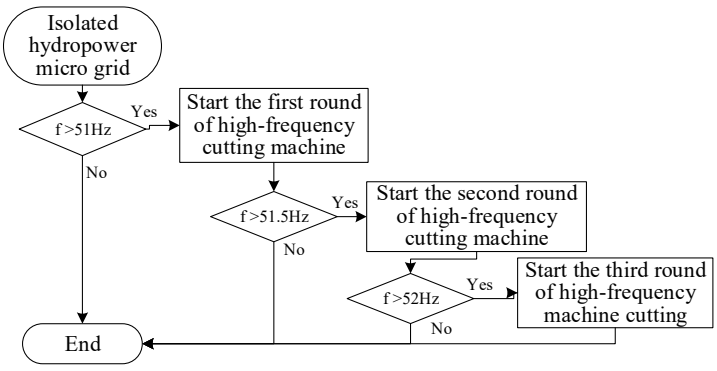


Figure 7. High-frequency generator-shedding flow after grid isolation in hydropower enriched area.

Based on the setting principles for hydropower unit high-frequency shedding schemes [21] and the scale of the simulation system, the high-frequency shedding device adopts a three-stage operation logic: the first stage triggers at 51.0 Hz, with subsequent stages increasing by 0.5 Hz (i.e., 51.5 Hz for the second stage and 52.0 Hz for the third stage).

The high-frequency cutting scheme is applied to the simulation model. According to the principle of capacity balance, the hydroelectric units of the small hydropower microgrid

are divided into four groups. Among them, the first group is composed of G6 and G10, with a capacity of 1.75 MW; the second group consists of G3 and G9, with a capacity of 1.94 MW; the third group consists of G4, G5, and G8, with a capacity of 2.26 MW; the fourth group consists of G1, G2, and G7, with a capacity of 1.925 MW. A small hydropower microgrid is set up to experience isolation at 5 s. The high-frequency cutting scheme for hydroelectric units initiates cutting at 51 Hz and operates in three rounds, with a stage difference of 0.5 s per round.

The simulation waveform is shown in Figure 8. After 5 s of isolating, the hydropower electromagnetic power suddenly decreases, but the mechanical power cannot suddenly change, leading to an increase in isolation frequency. At the time of 5.51 s, the isolated frequency reaches 51.0 Hz, which triggers the first power cut. The small hydropower microgrid cuts off the first group of hydropower units from the microgrid, tripping BRK6 and BRK10, resulting in a reduction of 1.75 MW in output. At 5.75 s, the second power cut is triggered when the frequency increases to 51.5 Hz. The system trips BRK4, BRK5, and BRK8 to cut off the third group of hydroelectric units, resulting in a reduction of 2.26 MW in output. At 6.04 s, the frequency increases to 52.0 Hz, triggering the third power cut. The system trips BRK1, BRK2, and BRK7, resulting in a reduction of 1.925 MW in output. After three rounds of machine cutting, the output of the hydroelectric unit remains the same as the local load, and stable operation can be maintained by adjusting the frequency of the unit itself. In the high-frequency cutting simulation, the highest frequency is 52.5 Hz, and the frequency drops to the steady-state value of 50.9 Hz 17 s after isolation.

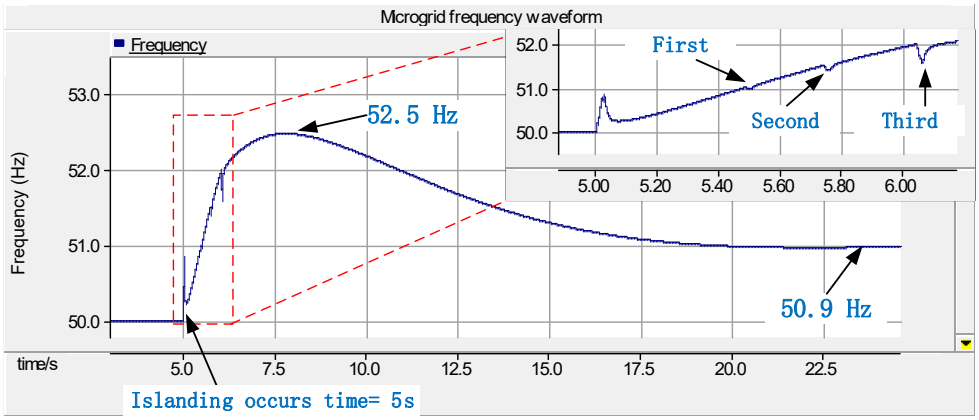


Figure 8. High-frequency cutting scheme simulation waveform diagram.

5.3. Centralized Decision + Local Control Generator-Shedding Strategy

In the proposed centralized decision-making + local control scheme, upon detecting an islanding event, the master station continuously issues grid-disconnection response plans to each substation, enabling the hydropower microgrid to respond promptly and maintain stable islanded operation. The microgrid refreshes islanding detection results every 20 ms; once islanding is confirmed, substations execute the pre-defined shedding plan from the master station, retaining critical units to supply local loads.

5.3.1. Generator-Shedding Strategy for Dry Seasons

During dry seasons, small hydropower microgrids transmit less power to the superior grid under normal operation. When islanding occurs, frequency rises rapidly, necessitating shedding operations to ensure stability and reliability.

Table 3 lists one shedding schemes for dry seasons. Scheme 4 was selected for analysis due to its ability to retain the maximum number of adjustable turbines. In dry sea-

sons, reduced water inflow lowers hydropower output, so priority is given to retaining critical loads.

Table 3. Centralized control machine cutting scheme during dry seasons.

Cutting	Reserve	Excess Power
L4, L5, L7, L8, L9, L10, L11, L14	G1, G2, G4, G5, G7, G8, G9, G10, L1, L2, L3, L6, L12, L13, L15	0.053 MW

Scheme 4 removes non-adjustable units G9, G10, adjustable unit G6, and loads L2, L3, L6, L7, L9, L10, L11, L15, with a total shedding capacity of 0.33 MW (note: G6 output is 0 MW in dry seasons). Compared to other schemes, Scheme 4 retains more adjustable turbines, facilitating full utilization of their regulating capacity.

Figure 9 show that when the system enters islanding at t = 5 s, the microgrid confirms islanding after a 20 ms detection cycle and executes load shedding (L4, L5, L7, L8, L9, L10, L11, L14) at 5.02 s. The remaining power surplus is only 0.053 MW, which is manageable via adjustable turbine regulation. The maximum frequency deviation during islanding is limited to 50.1 Hz, with a steady-state frequency of 50.06 Hz, meeting microgrid frequency fluctuation requirements and improving power supply reliability and quality.

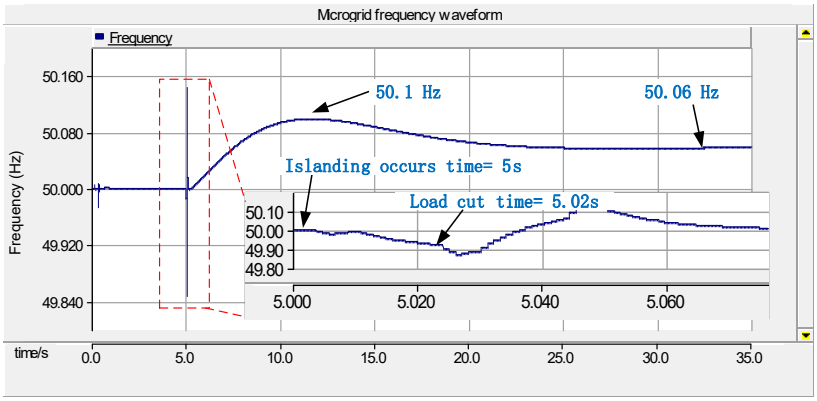


Figure 9. Simulation waveform diagram of centralized decision-making local control machine cutting scheme (during dry season).

5.3.2. Generator-Shedding Control for Wet Seasons

In wet seasons, increased water inflow raises hydropower output, leading to a larger power surplus during normal operation. When islanding occurs, frequency rises sharply, requiring shedding control to maintain stability via the centralized decision-making + local control scheme.

Table 4 presents shedding schemes for wet seasons, with all schemes achieving zero residual power and retaining the same number of loads. Scheme 1 was selected for analysis: it removes three adjustable turbines (G2, G3, G6) and two loads (L2, L3, L12), with a total shedding capacity of 3.675 MW.

Table 4. Centralized control machine cutting scheme during wet seasons.

Cutting	Reserve	Excess Power
G2, G3, G6, L2, L3, L12	G1, G4, G5, G7, G8, G9, G10, L1, L4, L5, L6, L7, L8, L9, L10, L11, L13, L14, L15	0 MW

Simulation results (Figure 10) show that when the system enters islanding at 5 s, the microgrid confirms islanding after a 20 ms detection cycle and executes the shedding command. Frequency rises temporarily after islanding but stabilizes rapidly post-regulation. After shedding, hydropower output matches load demand, and the remaining units' frequency regulation capability ensures stable operation. The maximum frequency during islanding reaches 50.2 Hz, dropping to a minimum of 50.115 Hz post-regulation and finally stabilizing at 49.9 Hz.

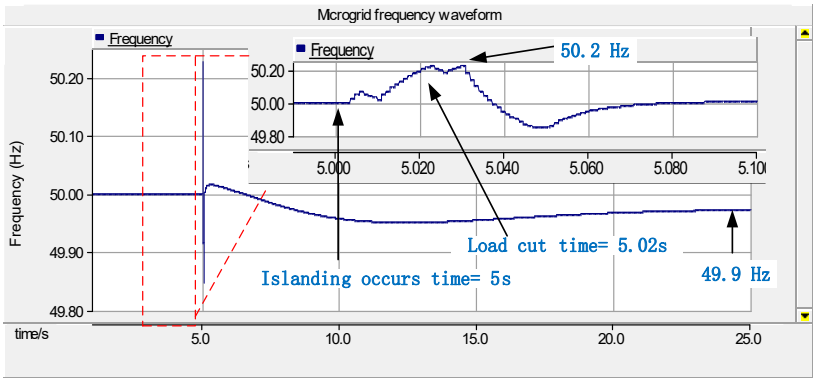


Figure 10. Simulation waveform diagram of centralized decision-making local control machine cutting scheme (during wet season).

5.4. Comparative Analysis

A comprehensive comparison of simulation results indicates that the master station centralized decision-making + substation local control scheme outperforms the traditional high-frequency shedding scheme in technical performance. Specifically, its real-time responsiveness and precision in load/generator shedding are significantly superior to those of the traditional approach.

6. Conclusions

In hydropower-rich regional grids, sudden islanding events can be managed via control technologies to form stable microgrids, enabling continuous power supply to local loads. As power-exporting systems, these grids are prone to excessive frequency elevation during islanding due to trapped surplus power.

Through theoretical analysis, this study identifies conditions for seamless microgrid transition during islanding and proposes a master station centralized decision-making + substation local control shedding strategy. Comparative theoretical and simulation analyses confirm that this strategy outperforms traditional high-frequency tripping schemes in frequency control effectiveness.

The proposed hierarchical framework addresses frequency instability in small hydropower microgrids under weak communication conditions, enhancing the precision and timeliness of load/generator shedding. It provides a practical technical solution for stable operation in remote regions with limited communication infrastructure.

Author Contributions: Author Contributions: Conceptualization, Z.C. and Z.Z.; methodology, Z.C.; software, Y.T. and Z.L.; validation, Z.C., Y.T. and Z.L.; formal analysis, Z.C.; investigation, Z.C.; resources, Z.Z.; data curation, Y.T. and Z.L.; writing—original draft preparation, Z.Z.; writing—review and editing, Z.Z.; visualization, Y.T. and Z.L.; supervision, Z.Z.; project administration, Z.C.; funding acquisition, N.S. All authors have read and agreed to the published version of the manuscript.

Funding: This research was funded by the project entitled 'Research on Intelligent Control Technology and Core Equipment Development of Renewable Energy Adapting to New Power Systems' (Project

No. 220728156271892) and the Guangdong Provincial Ordinary University Characteristic Innovation Project entitled 'Stability Analysis and Control Strategy of DC Microgrid Clusters Considering Time-Varying Topology' and the project 'Study on Multi-Objective Optimization of Microgrids Under Stability Constraints'. The APC was funded by the authors.

Institutional Review Board Statement: Not applicable (as our study does not involve humans or animals).

Informed Consent Statement: Not applicable (as our study does not involve humans).

Data Availability Statement: All data used in this study are presented within the article, and no additional external datasets were generated or analyzed. Therefore, no further separate data are available for sharing.

Conflicts of Interest: Author Zhanhong Liang was employed by the CLP Power Hong Kong Ltd. The remaining authors declare that the research was conducted in the absence of any commercial or financial relationships that could be construed as a potential conflict of interest.

References

1. Quintero, S.X.C.; Jiménez, J.D.M.; Aramburo, S.A. Feasibility of intentional islanding operation with small hydropower plants. In Proceedings of the 2012 Sixth IEEE/PES Transmission and Distribution: Latin America Conference and Exposition (T&D-LA), Montevideo, Uruguay, 3–5 September 2012.
2. Zhang, Z.; Yang, X.; Wang, Z.; Chen, Z.; Zheng, Y. Highly applicable small hydropower microgrid operation strategy and control technology. *Energy Rep.* **2020**, *6*, 3179–3191. [CrossRef]
3. Olatunde, O.; Hassan, M.Y.; Abdullah, M.P.; Rahman, H.A. Hybrid photovoltaic/small-hydropower microgrid in smart distribution network with grid isolated electric vehicle charging system. *J. Energy Storage* **2020**, *31*, 101673. [CrossRef]
4. Ren, Y.; Ren, L.; Zhang, K.; Liu, D.; Yao, X.; Li, H. Research on the operational strategy of the hybrid wind/PV/Small-Hydropower/Facility-Agriculture system based on a microgrid. *Energies* **2022**, *15*, 2466. [CrossRef]
5. Meyer, J.; von Solms, S. Design Considerations for Reducing Battery Storage in Off-Grid, Stand-Alone, Photovoltaic-Powered Cold Storage in Rural Applications. *Energies* **2022**, *15*, 3468. [CrossRef]
6. Rahman, M.; Hassan, N.; Khan, M.Z.R. Design of a Low Power Off-Grid Photovoltaic Water Pumping System for Rural Areas. In Proceedings of the 2020 11th International Conference on Electrical and Computer Engineering (ICECE), Dhaka, Bangladesh, 17–19 December 2020.
7. Oladigbolu, J.O.; Ramli, M.A.; Al-Turki, Y.A. Feasibility study and comparative analysis of hybrid renewable power system for off-grid rural electrification in a typical remote village located in Nigeria. *IEEE Access* **2020**, *8*, 171643–171663. [CrossRef]
8. Lan, Z.; Diao, W.; Tu, C.; Xiao, F.; Guo, Q. Research on hybrid operation mode and power coordination strategy of island microgrid with energy storage and hydrogen fuel cell. *Power Syst. Technol.* **2022**, *46*, 156–164.
9. Li, Z.; Zhang, M.; Zhang, J. Stability analysis and improvement of frequency cooperative control strategy for island microgrid considering time delay. *J. Tianjin Univ. Sci. Technol.* **2022**, *55*, 1061–1070.
10. Odou, O.D.T.; Bhandari, R.; Adamou, R. Hybrid off-grid renewable power system for sustainable rural electrification in Benin. *Renew. Energy* **2020**, *145*, 1266–1279. [CrossRef]
11. Khamis, A.; Khatib, T.; Yosliza, N.A.H.M.; Azmi, A.N. Optimal selection of renewable energy installation site in remote areas using segmentation and regional technique: A case study of Sarawak, Malaysia. *Sustain. Energy Technol. Assess.* **2020**, *42*, 100858. [CrossRef]
12. Guan, Y.; Vasquez, J.C.; Guerrero, J.M.; Wang, Y.; Feng, W. Frequency stability of hierarchically controlled hybrid photovoltaic-battery-hydropower microgrids. *IEEE Trans. Ind. Appl.* **2015**, *51*, 4729–4742. [CrossRef]
13. Xiong, X.; Ming, W.; Yu, J.; Zhenhao, S. Secondary Frequency Regulation Strategy of Virtual Synchronization Technology Based Microgrid Considering the Integrated Benefit. In Proceedings of the 2021 4th International Conference on Energy, Electrical and Power Engineering (CEEPE), Chongqing, China, 23–25 April 2021.
14. Khodaparastan, M.; Vahedi, H.; Khazaeli, F.; Oraee, H. A novel hybrid islanding detection method for inverter-based DGs using SFS and ROCOF. *IEEE Trans. Power Deliv.* **2015**, *32*, 2162–2170. [CrossRef]
15. Gupta, P.; Bhatia, R.S.; Jain, D.K. Active ROCOF relay for islanding detection. *IEEE Trans. Power Deliv.* **2016**, *32*, 420–429. [CrossRef]
16. Brogan, P.V.; Best, R.J.; Morrow, D.J.; McKinley, K.; Kubik, M.L. Effect of BESS response on frequency and RoCoF during underfrequency transients. *IEEE Trans. Power Syst.* **2018**, *34*, 575–583. [CrossRef]

17. Krzemianowski, Z.; Kaniecki, M. Low-head high specific speed Kaplan turbine for small hydropower—Design, CFD loss analysis and basic, cavitation and runaway investigations: A case study. *Energy Convers. Manag.* **2023**, *276*, 116558. [CrossRef]
18. Elewa, K.; Alhasheem, M.; Elhelw, H.M. Microgrid Applications: Effects of Communication Systems on Secondary Control Performance. In Proceedings of the 2023 5th International Youth Conference on Radio Electronics, Electrical and Power Engineering (REEPE), Moscow, Russia, 20–22 April 2023; pp. 1–6.
19. Mi, Y.; Deng, J.; Wang, X.; Lin, S.; Su, X.; Fu, Y. Multiagent Distributed Secondary Control for Energy Storage Systems With Lossy Communication Networks in DC Microgrid. *IEEE Trans. Smart Grid* **2023**, *14*, 1736–1749. [CrossRef]
20. Ahmed, M.; Meegahapola, L.; Vahidnia, A.; Datta, M. Stability and control aspects of microgrid architectures–a comprehensive review. *IEEE Access* **2020**, *8*, 144730–144766. [CrossRef]
21. Chen, Z.; Zhou, R.; He, J.; Mai, D.; Zhang, Z.; Luo, Y. Research on Unit Removal Method Under Islanding Operation of Small Hydropower Microgrid. In Proceedings of the 2021 IEEE 5th Conference on Energy Internet and Energy System Integration (EI2), Taiyuan, China, 22–24 October 2021.

Disclaimer/Publisher's Note: The statements, opinions and data contained in all publications are solely those of the individual author(s) and contributor(s) and not of MDPI and/or the editor(s). MDPI and/or the editor(s) disclaim responsibility for any injury to people or property resulting from any ideas, methods, instructions or products referred to in the content.